



The Open Electrical & Electronic Engineering Journal

Content list available at: www.benthamopen.com/TOEEJ/

DOI: 10.2174/1874129001711010087



RESEARCH ARTICLE

Modeling and Simulation of Variable Speed Variable Frequency Electrical Power System in More Electric Aircraft

Kelu Xu^{1,*}, Ning Xie¹, Chengmin Wang¹ and Xudong Shi²¹School of Electronic Information and Electrical Engineering, Shanghai Jiao Tong University, Shanghai 200240, China²Aeronautical Automation School, Civil Aviation University of China, Tianjin 300300, China

Received: November 11, 2016

Revised: February 10, 2017

Accepted: February 17, 2017

Abstract: The More Electric Aircraft (MEA), Variable Speed Variable Frequency (VSVF) and Electrical Power System (EPS) has larger generating capacity and higher energy efficiency than the conventional Constant Speed Constant Frequency EPS, but the generators of MEA have to work as redundant power supplies to improve the power supply reliability, instead of parallel power supply. To study the steady state operation and power source change strategies under different fault conditions of VSVF EPS, the integrated structure of VSVF EPS is firstly illustrated and operating principles of components are theorized. The key components including variable frequency generators, Bus Power Control Unit, rectifiers and other supplementary elements are then simulated to build a comprehensive VSVF EPS model on the platform of Simulink and the power source change strategies are realized by logic units. Finally, the stability analysis in terms of normal operation is carried out in case studies and power source exchange strategies in different situations are summarized. The results show that the model proposed by the paper can be used to simulate MEA VSVF EPS and analyze its whole operational process effectively and efficiently.

Keywords: More Electric Aircraft (MEA), Power system, Variable Speed Variable Frequency (VSVF), Modeling and simulation, Steady-state analysis, Power Source Exchange.

1. INTRODUCTION

The generating capacity of the conventional aircraft is relatively small, so some equipments have to be driven by hydraulic or pneumatic systems. The existence of hydraulic and pneumatic systems need many valves and control devices, which make the aircraft burdensome and unreliable. With the development of MEA VSVF EPS, the Engine Bleed Air System has been removed and the generating capacity of the EPS has greatly increased. Equipments that used to be driven by hydraulic or pneumatic systems such as environmental controls and wing anti-ice are partly supplied by electric system now [1]. Reducing hydraulic and pneumatic systems can simplify the design and maintenance of the aircraft, decrease the operational cost and improve the fuel efficiency. However, the increasing use of power electronics and electric-driven devices make the EPS of MEA much more complicated and thus impose a big challenge for its modeling and simulation, especially the difficulty in improving the simulation speed in case of large-scale model based on detailed components [2].

The conventional aircrafts generally have 2 generators and employ the Constant Speed Constant Frequency (CSCF) EPS. These 2 generators work in parallel power supply way to improve the reliability of EPS. The MEA has optimized the structure of generators by abolishing the Constant-Speed Drive (CSD) and employs a Variable Frequency Starter Generator (VFSG), whose frequency is in proportion to the speed of the engine. This structure observably improves the generating capacity and makes the VFSG more reliable than the conventional generator, but also lead to a failure in parallel power supply between these VFSGs. Because the frequency of VFSGs is not always the same, the generators of

* Address correspondence to this author at the School of Electronic Information and Electrical Engineering, Shanghai Jiao Tong University, Shanghai 200240, China; Tel: +86-13818836927; E-mails: xutad@foxmail.com; xutad@sjtu.edu.cn

MEA have to work in an independent way to supply the EPS. To ensure the reliability of EPS, one VFSG works as a backup power source for another VFSG, that means the operational mode of MEA is different from the conventional aircraft. To study the reliability of MEA EPS, the power supply status under different fault conditions must be considered. But recently, a large number of research on aircraft EPS modeling are focused on conventional aircrafts, and only a few researchers devoted to the research on MEA. But they still focused on either component-wise level, such as Transformer Rectifier Unit (TRU) [3], generators and various kinds of power conversion devices [4], or system-wise level of small-scale. For example, Griffio *et al.* built a model to analyze the stability of a MEA hybrid power system [5]. The model only simulated a single-generator (one-line) system that consisted of a synchronous generator and an 18-pulse rectifier. The fuel cell/battery and Auxiliary Power Unit (APU) were further considered in [6, 7]. These studies made a big progress in modeling the “more electric” EPS but still couldn’t show the “variable frequency” characteristic of MEA.

Based on a functional modeling approach in [2], this paper builds a comprehensive model for the VSVF EPS and use it to analyze the stability of MEA. The key components including generators, rectifiers, loads, breakers, control devices, cables and other supplementary elements are modeled from the system's point of view and the switching strategies of power sources in different situations are discussed. The stability analyses in terms of normal operation and different faults are carried out to study the applicability of this model for the VSVF MEA EPS.

2. STRUCTURE OF MEA VSVF EPS

B787 is the most typical MEA model at present. This paper illustrates the overall EPS structure according to its functional principles as shown in Fig. (1).

2.1. Structure of B787 EPS

The power sources of B787 are composed of four VFSGs, two APU Starter Generators (ASGs) and one Ram Air Turbine (RAT) generator. VFSGs are the main generators providing power for the electronic equipment during the normal flight while ASGs and RAT work as the backup power sources. These 4 VFSGs supply 4 independent 230VAC bus bars under the control of Generator Bus Breakers(GCBs).

230VAC bus bars (with frequency range of 380 - 800Hz) are the primary bus bars to supply all the electronic equipment through the power distribution system. From there, the power produced by the VFSG is either directly distributed to AC loads or transformed to three voltage levels: one is the secondary 115VAC by the Auto Transformer Unit (ATU); the other two are 270VDC by the Auto-Transformer Rectifier Unit (ATRU) and 28VDC by the Transformer Rectifier Unit (TRU) respectively. As shown in Fig. (1), the EPS of B787 is left-right symmetric with two 230VAC bus bars, two 270VDC bus bars, one 115VAC bus bar and one 28VDC bus bar on each side.

230VAC bus bars are so much important in the MEA VSVF EPS, once one of the 230VAC bus bar is out of service, all devices connected to this bus bar will lose power. In order to guarantee the power supply reliability, there exist some Bus Tie Breakers (BTBs) between these 4 230VAC bus bars. The function of BTB is to transfer the power-off 230VAC bus to the nearby available bus bar when some VFSG out of service (*e.g.* once VFSG_L1 breaks down, 230VAC_L1 bus bar and its loads will lost power. Closing L3_BT B can transfer these loads to 230VAC_L2, which is supplied by VFSG_L2). BTBs are controlled by the Bus Power Control Unit (BPCU). The dotted lines connecting BPCU and BTBs in Fig. (1) represent the control signals of BTBs, not the real electric connections.

This VSVF structure makes B787 an advanced more electric aircraft. Among all power source systems having been designed so far, VSVF is the most efficient one because of its simplified structure of the generator and reduced procedure of the energy conversion. The total generating capacity of B787 is 1450KVA, nearly four times that of other Boeing models. This large generating capacity makes the EPS extremely reliable. A test showed that B787 could fly on one engine for 5.5 hours with five of six generators turned off, which demonstrated the robustness of its EPS [8].

2.2. Structure of VFSG

The 115V/400Hz CSD generator was used on the conventional aircraft and the existence of CSD makes the generator complicated and heavy. To improve the generating capacity and power-to-weight ratio, VFSG has abolished the CSD and greatly reduced the weight of the generator.

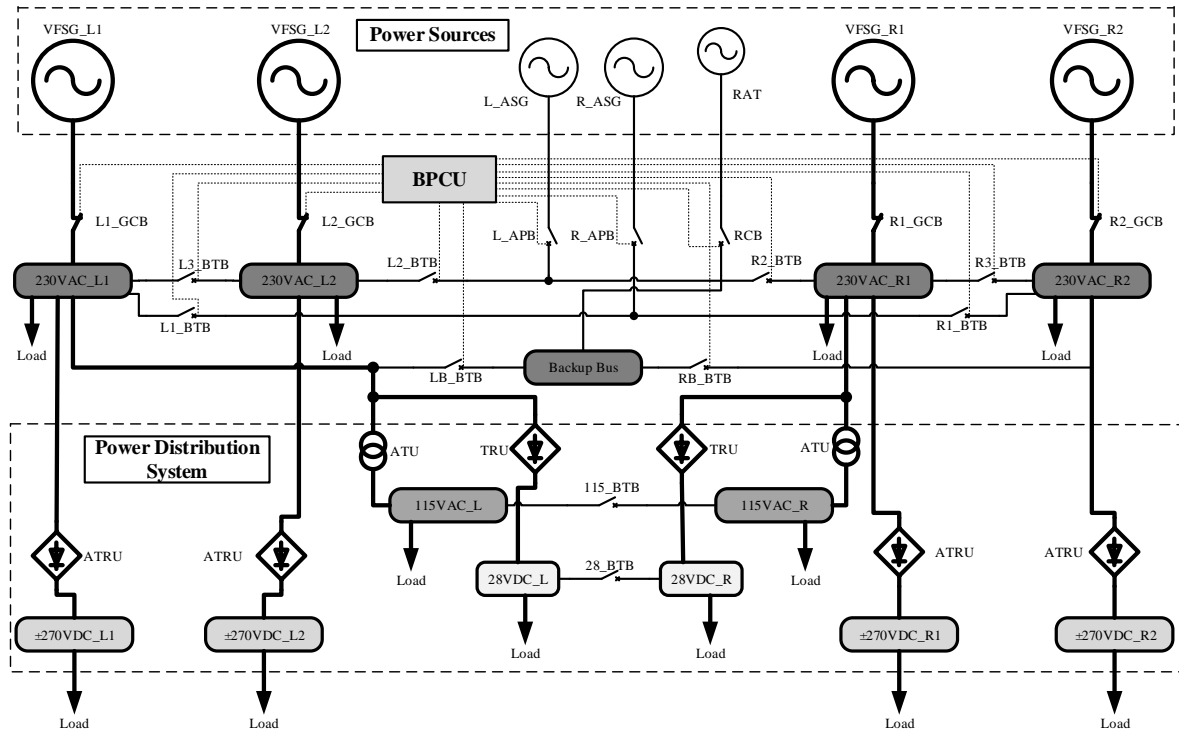


Fig. (1). Electrical Power System structure of B787.

VFSG is a 3-level brushless generator whose structure is shown in Fig. (2). The Exciter, powered by the Permanent Magnet Pilot Exciter, provides exciting current to the Main Generator through the Rotating Rectifier Assembly, which is installed on the rotor of Exciter and thus the 3-level generator is “brushless”. Through the voltage measurement and voltage regulator, the output voltage can be directly controlled by adjusting the exciting current. The VFSG provides variable frequency AC power to the aircraft power system under the control of GCB. Once the VFSG break down or the power quality of generator can’t satisfy the requirement of the EPS, GCB will cut down the connection between VFSG and EPS to ensure the safety of other equipment.

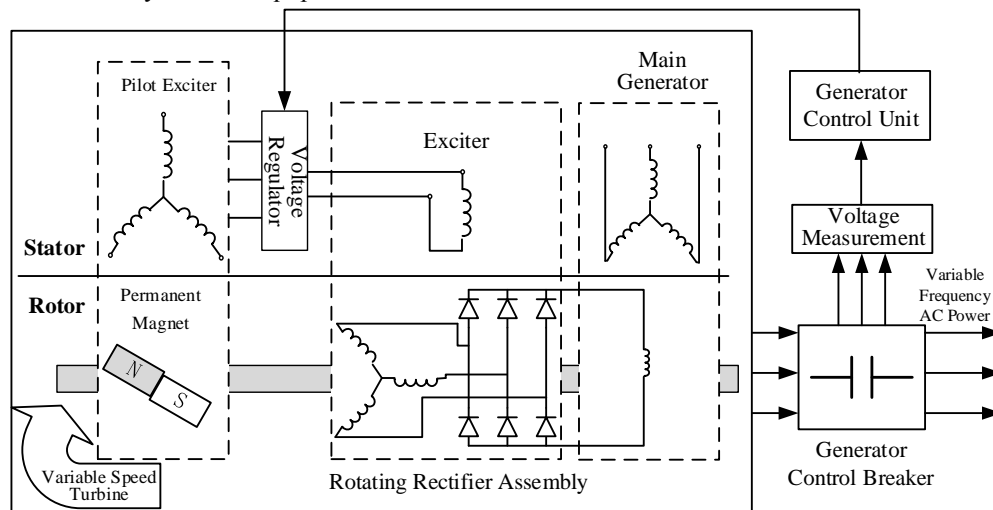


Fig. (2). 3-level brushless generator structure.

2.3. Operation Principle of BPCU

As mentioned above, BPCU is the control center of BTBs and it realizes the power transfer functions by switching on/off the breakers including BTBs, Auxiliary Power Breakers (APBs), and RAT Control Breaker (RCB). In a normal flight, all the BTBs are off and the system operates in a 4-line isolated configuration. When an accidental event results in a VFSG failure, BPCU will switch on the related BTB to transfer associated loads to the available generators. If 3 or

more VFSGs are out of service, BPCU will switch on APBs to put the ASGs into operation, satisfying the load demand on the aircraft. In the worst case, all VGSGs and ASGs break down, BPCU will switch on RCB, using the RAT generator as the last power source to ensure the flight landing.

The practical structure of BPCU is very complex and it contains many integrated cells and control devices. It is very difficult to simulate the structure of BPCU integrally and it is also not necessary. If a functional model can realize the power source change function of BPCU, it can be used as a useful tool to represent the BPCU.

2.4. Structure of Rectifiers

Rectifiers (ATRU and TRU) on MEA are normally 12-pulse configuration and usually employ uncontrolled rectifiers [9]. Fig. (3) shows a schematic of a 12-pulse rectifier circuit which employs a three-winding isolation transformer with a Y-Y- Δ connection. An inter-phase reactor (L) is added to connect two rectifiers in parallel. When the output voltages of the two converters are equal, the inter-phase reactor is transparent. However, when the output voltages of the converters are not equal, the winding of the inter-phase reactor presents sufficient inductance to support the voltage imbalance [10]. Due to the existing of power converters, the system contains a lot of harmonics. Filters on the AC side are needed to meet the standards of harmonic contents.

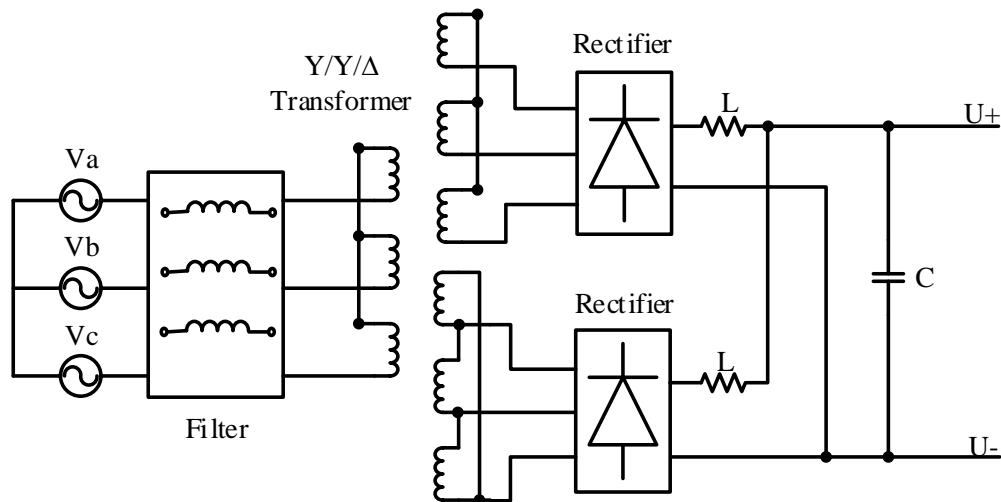


Fig. (3). 12-pulse Y-Y- Δ diode rectifier.

3. MODELING OF MEA EPS

Many researchers have built models for the EPS of MEA to study its performance like power quality or stability. The models are usually as simple as a single-generator system and their structure won't change with different working situations of the aircraft. In our study, the complete structure of the most complex MEA B787 is modeled; and the EPS structure will be changed with different switching strategies of the power sources as requested by the flight.

This section describes the modeling of MEA EPS components based on the scheme drawn in Fig. (1) in detail. They are generators (VFSG, ASG and RAT), breakers (BTB, GCB, APB and RCB), BPCU, ATRU, AC/DC loads, cables, and other supplementary elements (*e.g.*, measurements). The modeling focuses on the components' functionality instead of on their detailed structures. The comprehensive model is built on the platform of MATLAB/Simulink and the built-in blocks provided by Simulink are used as many as possible to save the simulation time.

3.1. The Model of Generators

The VFSG simulation model is shown in Fig. (4). Module "Speed" is a programmable signal that can imitate the variable speed of the turbine (so-called "variable frequency"). Module "Generator" is a simplified generator subsystem and module "GCU" contains the exciting system and voltage regulator. Module "GCB" controls the output voltage of the generator and there is a signal status tag in it to represent the working state of this VFSG (*e.g.*, the tag "L1_GCB" will become FALSE if VFSG_L1 breaks down). The performance of the output voltage is stable and suitable for the B787 EPS.

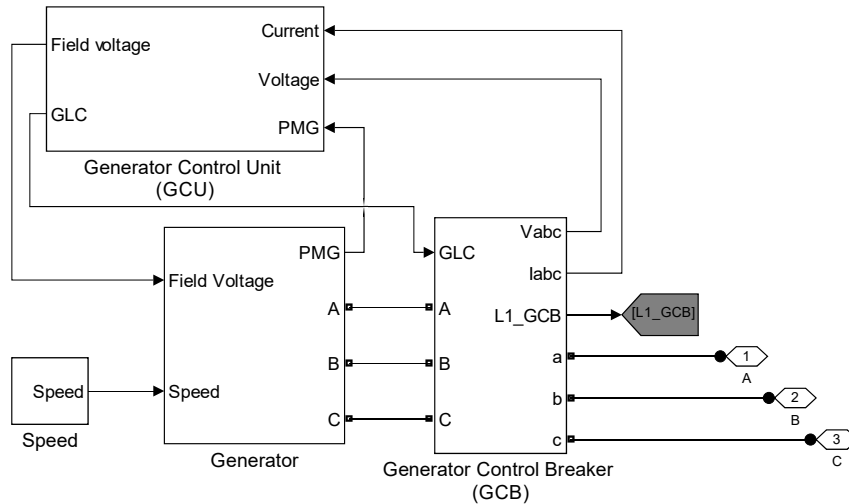


Fig. (4). VFSG simulation model.

To achieve the voltage stability of the generator, the voltage regulator in “GCU” employs the soft excitation current feedback mode to adjust the output voltage. The voltage regulator model is shown in Fig. (5).

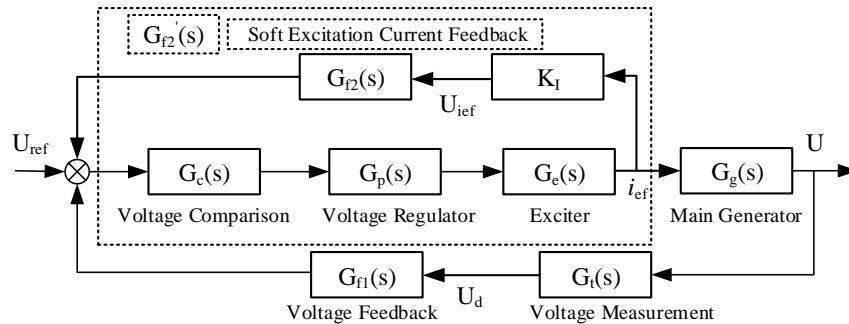


Fig. (5). Voltage regulator model.

U_{ref} is the reference voltage, usually 230V. The equivalent transfer function of the soft excitation current feedback link is $G'_{r2}(s)$;

$$G'_{r2}(s) = \frac{G_c(s)G_p(s)G_e(s)}{1 + G_c(s)G_p(s)G_e(s)K_fG_r2(s)} = \frac{(T_1s + 1)(T_e s + 1)}{(\alpha^{-1}T_1s + 1)(\alpha T_e s + 1)} \tag{1}$$

The transfer function of the voltage measurement is:

$$G_t(s) = \frac{K_t}{T_r s + 1} \tag{2}$$

The transfer function of the voltage feedback is:

$$G_f(s) = \frac{(T_2 - T_1)s + 1}{T_1 s} \tag{3}$$

Where T_1, T_2 are the time constant of the voltage comparison, α is the amplification factor of the voltage regulator, T_e is time constant of the exciter, K_t and T_r are the amplification factor and time constant of the voltage measurement.

Fig. (4) shows the simulation model of VFSG, although the structures of ASG and RAT are different from that of VFSG, they are simple power sources. So they can be modeled in the same way as shown in Fig. (4) with a constant speed of 12000r/min (i.e., 400Hz).

3.2. The Model of Breakers

Buses are connected together through BTBs. In the event that one generator should fail it is automatically isolated from its respective bus and all associated loads are taken over by the operative generator. A controlled three-phase breaker can achieve this function.

The model of L3_BTBT which combines 230VAC_L1 Bus and 230VAC_L2 Bus is shown in Fig. (6). The tag “L3_BTBT” is the control signal of this breaker. When one of the left generators turn off, the control signal status becomes TRUE and breaker will switch on to transfer the power source. To avoid the error operations, a time delay block was added in this model. The breaker won't close unless the control signal keeps TRUE for at least 0.5s.

The output of the generators are controlled by the GCB, APB and RCB. These breakers can share this BTBT model because they function in the same way. A given disable signal can cut off the generator from the EPS to imitate the generator fault in a simple way.

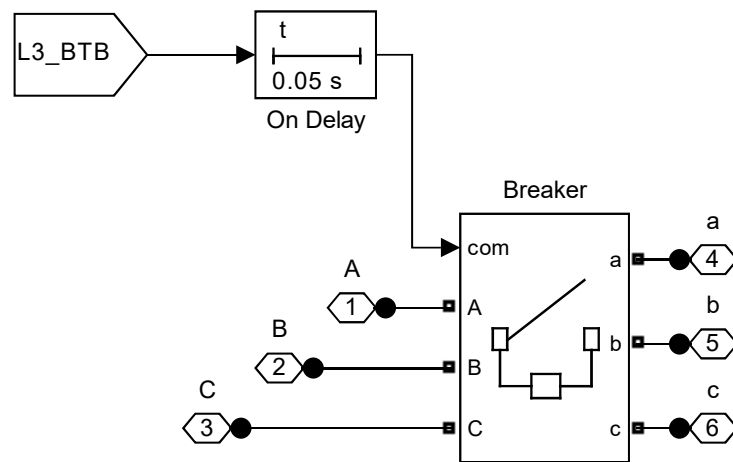


Fig. (6). L3_BTBT model.

3.3. The Model of BPCU

BPCU is used to realize the switchover between the power sources under different conditions by controlling the BTBs. When three or more generators turn off, the ASG starts up and some power-off devices must be transferred to the backup power sources. When some of the generators turn off, BPCU would close the corresponding BTBs according to a given strategy. The logic elements were used to implement the switching function. Fig. (7) shows parts of the BPCU logic elements to control 6 of the BTBs. The purpose of this module is to create the power switch strategy under different generator fault conditions, by building a logical relations between the generators working states (*i.e.* the signal status of GCBs) and the control signals of BTBs.

For example, if VFSG_L1 fails, meaning the state of logic tag “L1_GCB” is FALSE, then the logic tag “K2” becomes TRUE, which will lead to the logic tag “L3_BTBT” becoming TRUE. The logic tag “L3_BTBT” is the control signal of “L3_BTBT”, so L3_BTBT will close on to transfer the power-off 230VAC_L1 Bus loads to the 230VAC_L2 Bus. This is just one simple example of the power switch strategy to realize the power sources change function of BPCU. Other BTBs work at the same way. By judging the different signal status of GCBs, BPCU can manipulate the control signals of all BTBs through the power switch strategy to switch the power sources under different fault conditions.

By changing the working state of the generators, BPCU can imitate the other different generator-fault situations. Because of using the basic logic elements in the Simulink platform, this BPCU model has a quick response ability.

3.4. The Model of ATRU (TRU)

Referring to the modeling and simulation process of 12-pulse ATRU in [10], The final ATRU (TRU) model is shown in Fig. (8). It consist of one filter, one three-phase Y-Y-Δ transformer, two rectifiers, two inter-phase reactors and one filter capacitor. The following two formulas can be used to calculate the inter-phase reactor and the DC capacity of the ATRU:

$$L = \frac{\sqrt{2}(1-\frac{\sqrt{3}}{2})V_l}{3\omega I_{d\min}}, \quad C = \frac{2}{2\pi f R_{ef}} \tag{4}$$

Where, V_l is the input line voltage and $V_l = \frac{\pi}{3\sqrt{2}}V_d$. V_d is the desired DC voltage. $I_{d\min}$ is the minimum load current, nearly 1% of the DC current. R_{ef} is the equivalent resistance on DC side.

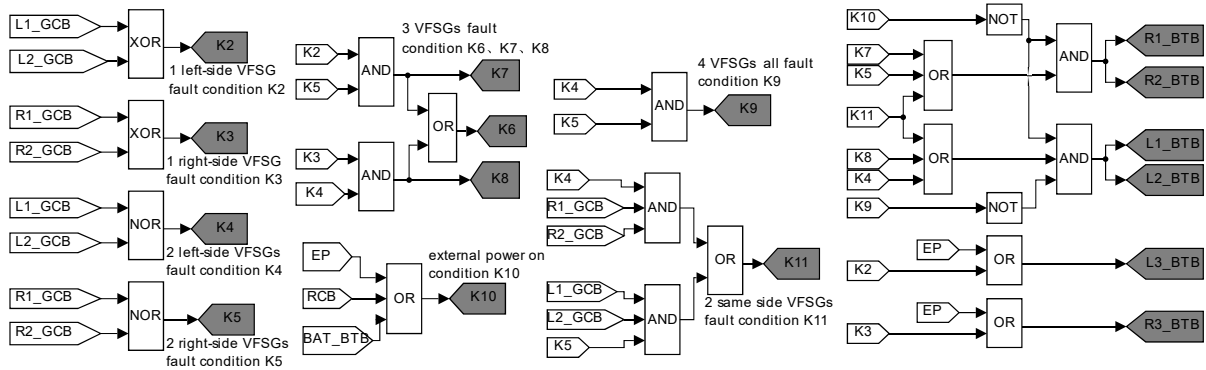


Fig. (7). Parts of BPCU model.

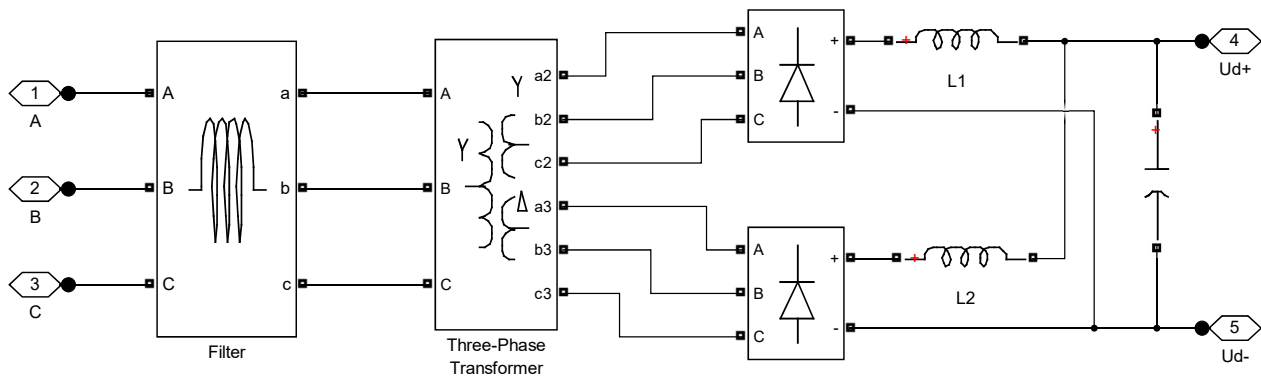


Fig. (8). ATRU (TRU) model.

3.5. Loads, Cables, and Other Supplementary Elements

There are many kinds of loads in the MEA power system but in this study, different types of loads are not considered. Assume that the power-factor of AC loads is constantly 0.85 and all loads regard as PQ nodes, which data changing with different working periods.

MEA employs the three-phase four-wire system, neutral line on the airframe. The MEA lines are relatively short so we can ignore the capacitive in the PI-type equivalent model and directly represented as an equivalent impedance, using the experimental measured parameters.

Other supplementary elements like bus bars and measurements can be simply modeled by the built-in blocks of Simulink.

Finally, combined all the key component models referring to Fig. (1), the comprehensive MEA EPS model is finished. Though the scale of this comprehensive model is very large, it does not need too much computing time using the original Simulink models.

4. CASE STUDIES

This section will assess the performance of the comprehensive model for simulation study under two different conditions: the normal operation and the fault cases. The parameters for this study are list in Table 1 [11].

Table 1. The parameters of simulation.

Parameter	Value	Parameter	Value
Generator voltage	230Vrms	Speed of engine	11000~14000r/min
Cable resistance	3.71mΩ/m	Cable inductance	3.28nH/m
ATRU filter reactance	0.1mL	ATRU inter-phase reactor inductance	1.67mH
ATRU DC capacity	0.99mF	TRU filter reactance	1mL
TRU inter-phase reactor inductance	0.13mH	TRU DC capacity	13mF
230VAC total load	24.35KVA	115VAC total load	56.93KVA
270VDC total load	171.68KW	28VDC total load	22.62KW

4.1. Normal Operation

The loads of the MEA do not remain a constant value because the system have to change the power of different devices to adapt to the environment changes in flight. So the load disturbance of the MEA EPS in flight is a good method to verify the stability of this comprehensive model.

At the beginning, only half of loads are working. This process last for 2s and then at $t = 2s$, the other half loads are online and last for another 2s, then at $t = 4s$, the added half loads are removed and return to the initial state. In this case, all the BTBs are off and the system operates in a 4-line isolated configuration. Each single line is independent so we choose one of them to observe the simulation performance. The frequency of the output voltage of VFSG_R1 is shown in Fig. (9) and the response results of the 230VAC_R1 Bus and 270VDC_R1 Bus are shown in Fig. (10).

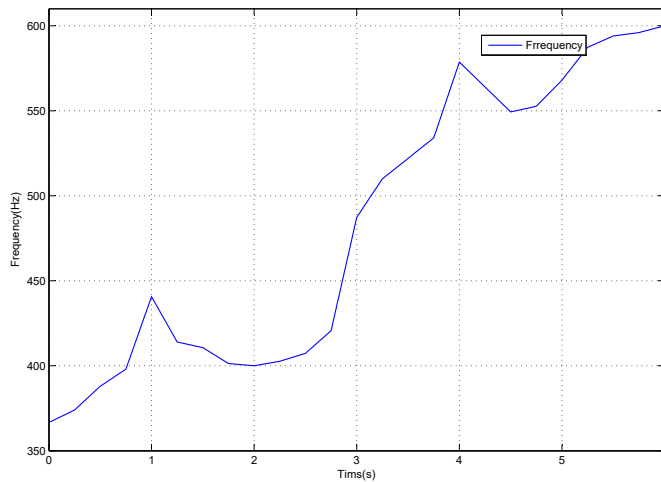


Fig. (9). The frequency of the output voltage of VFSG_R1.

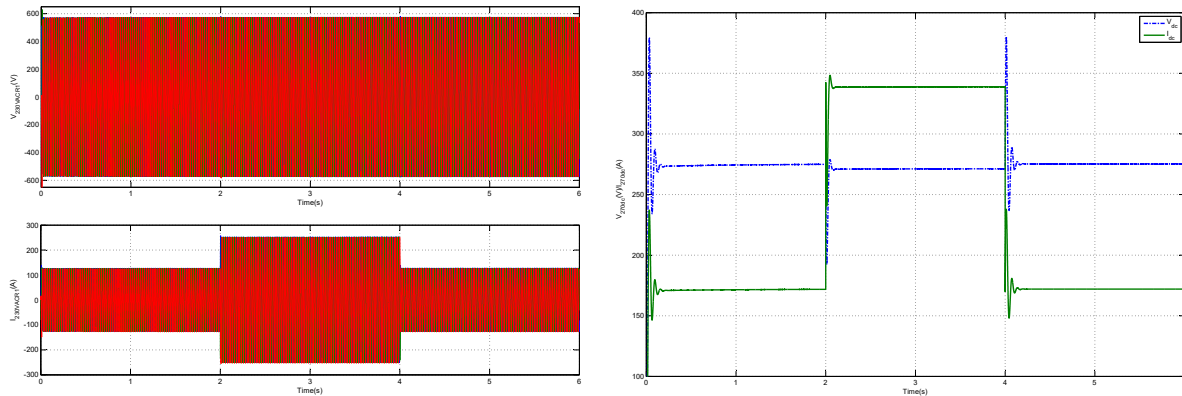


Fig. (10). Voltage and current of 230VAC_R1 Bus and 270VDC_R1 Bus when loads changing.

As can be observed, the “variable frequency” characteristic of the VFSG can be simply observed by the frequency waveform in Fig. (9). The frequency of the VFSGs is changing between 366 Hz to 600 Hz when the speed of generator changing between 11000 r/min to 18000 r/min. The Root Mean Square (RMS) line voltage of 230VAC Bus is 396.7V and it remains stable during the whole simulation. That shows a very well regulation performance of this generator mode. The current of 230VAC Bus has an obvious rise and fall following the increase and derating of loads. The simulation result of 230VDC_R1 Bus voltage in Fig. (10) shows that the ATRU models have a good dynamic response.

Other measurements shows the RMS line voltage of the 115VAC_R Bus is 200.9V and the THD of the current on the AC side is 3.68%. The voltage of 270VDC_R1 is 271V and 28VDC_R is 28.55V. These simulation results and the voltage ripples on DC side all meet the power quality standards of MIL-STD-704F in Tables 2 and 3 [12].

Table 2. MIL-STD-704F AC normal characteristics.

Steady state characteristics	230VAC	115VAC
Steady state Voltage/V	208 to 244	108 to 118
Voltage Unbalance/V	< 5.0	< 3.0
Current THD	< 5%	< 5%

Table 3. MIL-STD-704F DC normal characteristics.

Steady state characteristics	270VDC	28VDC
Steady state voltage/V	250 to 280	22 to 29
Ripple amplitude/V	< 6.0	< 1.5

This case demonstrates that the comprehensive model can accurately and effectively simulate the normal operation of MEA EPS and it's useful to study the stability analysis of MEA EPS.

4.2. Fault Case: Loss of VFSG(s)

As mentioned above, BPCU controls power transfer functions by switching on/off BTBs under different conditions. In this section, a series of fault cases will be assumed to observe the response of BPCU and the performance of some important buses.

The whole process is assumed that MEA EPS is running under normal operation in the initial state, then VFSG_L1 stop at t=2s, then VFSG_R1 stop sequentially at t=4s, finally VFSG_R2 stop too at t=6s. Run the simulation model and get the state of associated BTBs shown in Fig. (11), the response of 230VAC Bus bars shown in Fig. (12), and the response of 270VDC Bus bars shown in Fig. (13).

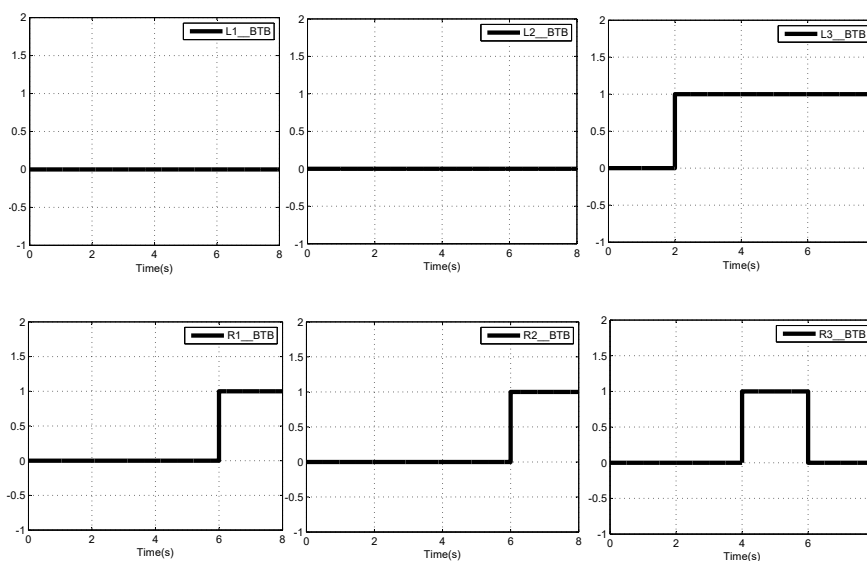


Fig. (11). State of BTBs consolidating the primary 230VAC Bus.

In initial state, the EPS is under normal operation, then a fault occurs in VFSG_L1 at $t=2s$ and this generator has to be disconnected from the system. Theoretically, at this moment, BPCU will switch on the L3_BTBT to transfer the loads powered by 230VAC_L1 Bus to 230VAC_L1 Bus. The state of L3_BTBT in Fig. (11) shows that the BPCU operates correctly. The voltage and current performance in Figs. (12 and 13) demonstrates that the 230VAC_L1 Bus had been taken over by VFSG_L2 after 0.5s delay.

At $t = 4s$, VFSG_R1 stopped. As Fig. (11) shows, R3_BTBT switched on and transferred the 230VAC_R1 Bus loads to 230VAC_R2 Bus. The voltage and current in Figs. (12 and 13) demonstrates this too.

Then at $t = 6s$, VFSG_R2 stopped too. Having three of four main generators out of service, the ASGs started to support the EPS. Using ASG_L to power the 230VAC_R1 Bus and ASG_R to power the 230VAC_R2 Bus, R1_BTBT and R2_BTBT switched on. Because the frequency of ASG_L and ASG_R are not accurately the same, R3_BTBT has to be switched off otherwise it would connect these two generators. The state of R3_BTBT demonstrates that BPCU had effectively finished the power transfer functions.

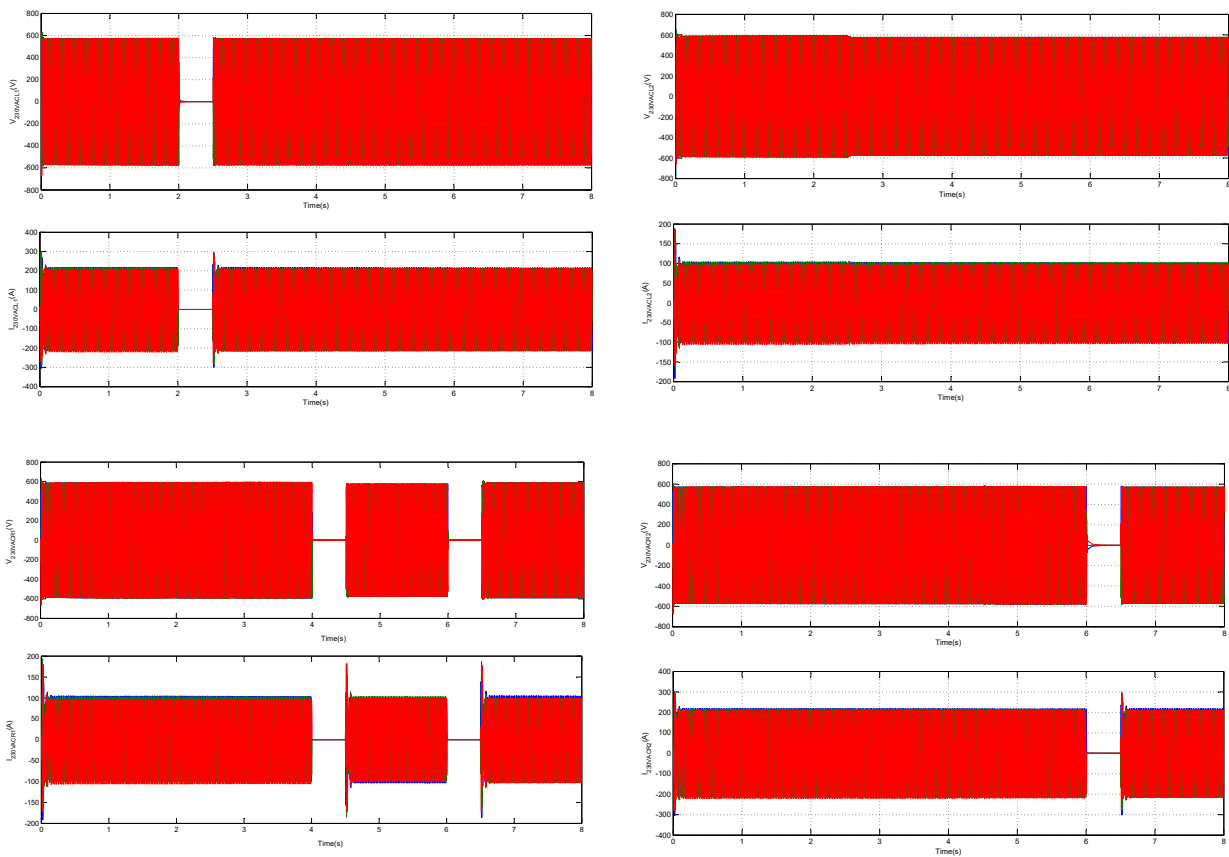


Fig. (12). Voltage and current of 4 primary 230VAC Bus during fault.

CONCLUSION

Compared with the conventional aircraft, MEA is lighter, easier to maintain and more efficient due to its hydraulic and pneumatic systems partially replaced by electric system. Having large generating capacity and advanced solid-state power distribution system, the EPS of MEA is reliable but complex. By means of functional modeling approach, a comprehensive Simulink model has been built to study the performance of the EPS in case of both normal conditions and different faults. The results showed that essential parameters meet the standards required by MIL-STD-704F under normal operation. Besides, the logic procedures representing the control strategies for switching power in case of different faults were implemented. The case study demonstrated that the system can be effectively recovered from different generator faults. All simulations were carried out within acceptable times.

Currently, this study only considers static AC and DC loads with dynamic loads neglected. The impacts of variable loads to MEA EPS along with the security analysis under different conditions will be addressed in the future work.

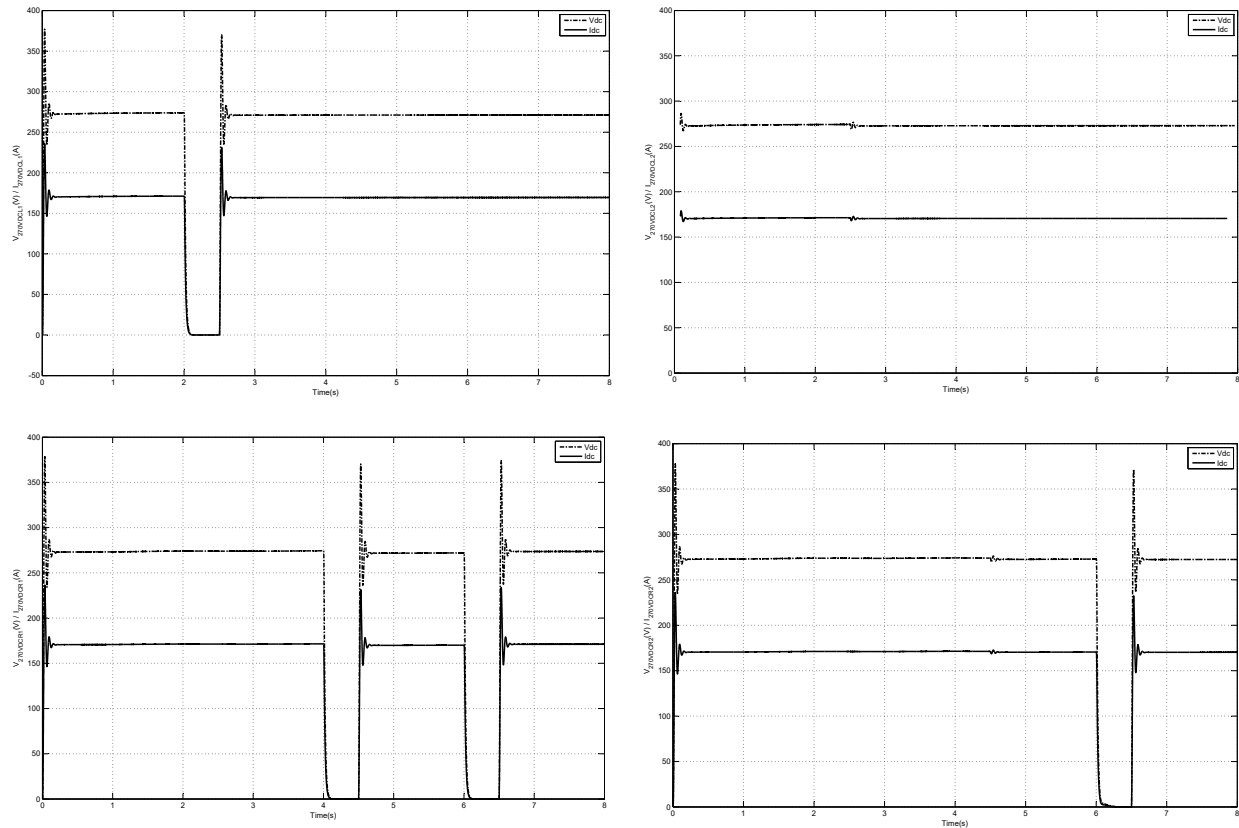


Fig. (13). Voltage and current of 270VDC_L1~R2 Bus during fault.

CONFLICT OF INTEREST

The authors confirm that this article content has no conflict of interest.

ACKNOWLEDGEMENTS

This work is supported by the National Natural Science Foundation of China (Grants nos. 51377161).

REFERENCES

- [1] J. A. Weimer, "Electrical power technology for the more electric aircraft", 2013. [http://dx.doi.org/10.1109/DASC.1993.283509]
- [2] T. Wu, S. V. Bozhko, and G. M. Asher, "Accelerated functional modeling of aircraft electrical power systems including fault scenarios", In: *Industrial Electronics, 2009. IECON '09. 35th Annual Conference of IEEE*, IEEE, 2009, pp. 2537-2544. [http://dx.doi.org/10.1109/IECON.2009.5415246]
- [3] A. O. Monroy, H. Le-Huy, and C. Lavoie, "Modeling and simulation of a 24-pulse Transformer Rectifier Unit for more electric aircraft power system", In: *Electrical Systems for Aircraft, Railway and Ship Propulsion (ESARS)*, IEEE, 2012, pp. 1-5. [http://dx.doi.org/10.1109/ESARS.2012.6387383]
- [4] Z. Yang, J. Qu, and Y. Ma, "Modeling and simulation of power distribution system in more electric aircraft", *J. Electr. Comput. Eng.*, vol. 2015, no. 8, pp. 1-7, 2015. [http://dx.doi.org/10.1155/2015/847624]
- [5] A. Griffo, and J. Wang, "Modeling and stability analysis of hybrid power systems for the more electric aircraft", *Electr. Power Syst. Res.*, vol. 82, no. 1, pp. 59-67, 2012. [http://dx.doi.org/10.1016/j.epr.2011.08.017]
- [6] A. Eid, H. El-Kishky, and M. Abdel-Salam, "Modeling and characterization of an aircraft electric power system with a fuel cell-equipped APU paralleled at main AC bus", In: *Power Modulator and High Voltage Conference*, IEEE, 2010, pp. 891-904. [http://dx.doi.org/10.1109/IPMHVC.2010.5958335]
- [7] A. Eid, H. El-Kishky, and M. Abdel-Salam, "Modeling and characterization of an aircraft electric power system with a fuel cell-equipped APU connected at HVDC bus", In: *Power Modulator and High Voltage Conference*, IEEE, 2010, pp. 639-642. [http://dx.doi.org/10.1109/IPMHVC.2010.5958440]

- [8] K.L. Xu, N. Xie, C.M. Wang, J.W. Deng, and X.D. Shi, "Static modeling and power flow of the more electric aircraft power system", In: *Systems and Informatics (ICSAI) 3rd International Conference*, IEEE, 2006, pp. 193-198.
[<http://dx.doi.org/10.1109/ICSAI.2016.7810953>]
- [9] G. Gong, M.L. Heldwein, and U. Drogenik, "Comparative evaluation of three-phase high-power-factor AC-DC converter concepts for application in future More Electric Aircraft", *IEEE Trans. Ind. Electron.*, vol. 52, no. 3, pp. 727-737, 2005.
[<http://dx.doi.org/10.1109/TIE.2005.843957>]
- [10] L. Han, J. Wang, and D. Howe, "State-space average modeling of 6 and 12 - pulse diode rectifiers", In: *European Conference on Power Electronics and Applications*, IEEE, 2007, pp. 1-10.
- [11] X. Xia, "*Dynamic Power Distribution Management for all Electric Aircraft*", School of Engineering MSc by Research Thesis, Cranfield University, 2011.
- [12] Z. Yang, J. Qu, Y. Ma, and X. Shi, "Modeling and simulation power distribution system in more electric aircraft", *J. Electric. Comp. Eng.*, vol. 2015, p. 67, 2015.
[<http://dx.doi.org/10.1155/2015/847624>]

© 2017 Xu et al.

This is an open access article distributed under the terms of the Creative Commons Attribution 4.0 International Public License (CC-BY 4.0), a copy of which is available at: <https://creativecommons.org/licenses/by/4.0/legalcode>. This license permits unrestricted use, distribution, and reproduction in any medium, provided the original author and source are credited.